

## Influence of Thermodiffusion on Time Dependent Casson Fluid Flow past a Wavy Surface

**B. Ramadevi<sup>1</sup>, J. V. Ramana Reddy<sup>2</sup>, V. Sugunamma<sup>3\*</sup>**

Department of Mathematics

S. V. U. College of Sciences, Tirupati, India

E-mails: <sup>1</sup>bujularamadevi92@gmail.com, <sup>2</sup>jvr.mrpk@gmail.com, <sup>3</sup>vsugunar@gmail.com

*\*Corresponding author*

(Received February 11, 2018; Accepted April 2, 2018)

### Abstract

The characteristics of unsteady motion of Casson fluid over a wavy surface with magnetic field is studied. The energy and diffusion equations are encompassed with radiation, heat source and thermo diffusion effects. The flow governing equations have been solved using regular perturbation technique. MATLAB bvp4c package is for discerning the impact of governing parameters on the usual flow profiles. various pertinent parameters on velocity, temperature and concentration profiles of the Casson fluid flow. The frictional factor, heat and mass transfer coefficients are tabulated for the same parameters. From this analysis, it is worth mentioning that a hike in fluid viscosity slowdowns the velocity profiles but the result is opposite with Soret effect. Also, accelerating values of radiation parameter uplifts the rate of mass and heat transport but controls the shear stress.

**Keywords-** Radiation, Soret number, MHD, Vertical wavy plate, Casson fluid.

### Nomenclature

$a^*$  : Amplitude of the wavy wall  
 $C_p$  : Specific heat capacitance  
 $C_w$  : Wall concentration  
 $C_\infty$  : Ambient concentration  
 $D$  : Molecular diffusivity  
 $F$  : Thermal radiation parameter  
 $Gc$  : Solutal and thermal Grashof numbers respectively  
 $h$  : A constant  
 $k$  : Thermal conductivity  
 $K$  : Porosity parameter  
 $M$  : Magnetic parameter  
 $n^*$  : Dimensional positive real constant  
 $p$  : Pressure gradient  
 $Pr$  : Prandtl number  
 $Q_0$  : Dimensional heat absorption coefficient  
 $Q_h$  : Heat absorption parameter  
 $Sc$  : Schmidt number  
 $Sr$  : Soret number  
 $T_w$  : Wall temperature

- $T_\infty$  : Ambient temperature  
 $u, v$  : Components of dimensional velocities along  $x, y$  – directions  
 $t^*$  : Dimensional time  
 $u_p$  : Dimensional moving velocity of the plate (dimensionless)  
 $U_p$  : Moving velocity of the plate  
 $\alpha_T$  : Heat source parameter  
 $\beta$  : Casson parameter  
 $\beta_C$  : Concentration expansion coefficient  
 $\beta_T$  : Thermal expansion coefficient  
 $\epsilon$  : Small positive constant less than unity  
 $\mu$  : Dynamic viscosity  
 $\nu$  : Kinematic viscosity  
 $\rho$  : Density  
 $\sigma$  : Electrical conductivity of the fluid

## 1. Introduction

The non-Newtonian fluids differ in characteristics compared to Newtonian fluids due to heavier viscosity. Some examples of non-Newtonian fluids are glue, paint, honey, tooth paste, corn flour paste, blood, shampoo, mud, chilli sauce, syrups, etc. Mostly the applications of non-Newtonian fluids are seen in biomechanics, chemical industries, geophysics, medicine, etc. Hameed and Nadeem (2007) analysed the flow characteristics of non-Newtonian fluid through a porous surface accounting Lorentz force. The impact of variable viscosity on mixed convection flow of non-Newtonian fluid past a vertical surface was studied by Jayanthi and Kumari (2007). Ramadevi et al. (2017) illustrated the comparative study for the MHD flow of two distinct non-Newtonian fluids due to stretching sheet with Cattaneo-Christov heat flux model. Sulochana et al. (2016) reviewed the power of Lorentz force on non-Newtonian fluid flows.

The Casson, Maxwell and Viscoelastic fluids are of different types in non-Newtonian fluids and which are used to perceive the behaviour of non-Newtonian fluids. Hayat et al. (2012) bestowed a series solution to address the flow characteristics of Casson fluid by considering magnetic field, cross diffusion. Mukhopadhyay (2013) reported the impact of heat transfer on the flow of Casson fluid past a non-linear stretched surface. The unsteady motion of MHD Casson fluid past a vertical oscillating plate with free convection was scrutinized by Khalid et al. (2015). The influence of pertinent parameters on velocity, concentration and temperature profiles for the MHD flow of Casson fluid with the presence of viscous-dissipation was obtained by Venkateswarlu et al. (2017). Megahed (2013) reported the numerical solution for velocity and temperature with the impact of variable heat flux and variable fluid properties on the flow of Maxwell fluid. Han et al. (2014) inspected the effects of heat transport on the coupled flow of viscoelastic fluid by using the model recommended by Christov and Cattaneo.

In unsteady flow problems, the governing equations consist of time derivatives also. Mustafa et al. (2011) used the homotopic procedure to find the influence of heat transfer in unsteady flow induced by a moving surface. A numerical study was conducted by Pushpalatha et al. (2017) for

the time dependent flow towards a convective surface in the presence of radiation and cross-diffusion.

The concept of magnetohydrodynamics is beneficial in engineering problems such as cooling of nuclear reactors, electromagnetic casting and plasma confinement etc. Also it is used in magnetic drug targeting. Due to these wider applications, Mahapatra and Gupta (2001) presented the solution for MHD flow (two dimensional) past a deformable sheet. To the extension of this Nadeem et al. (2013) considered steady three-dimensional flow via porous surface. Zhang et al. (2015) studied the MHD flow of nanofluids towards a flat plate in view of variable surface heat flux effects. Hayat et al. (2016) presented the characteristics of unsteady magnetohydrodynamic flow caused by stretching of a sheet with slip boundary conditions. Sulochana et al. (2017) examined the flow attributes of nanofluids in the presence of magnetic field.

The interchange of thermal energy between physical systems is known as heat transfer. The heat transfer rate depends on temperatures of the physical systems. Heat transfer occurs through convection, conduction, radiation and advection. Mostly, heat transfer is used in material processing, thermal management of electronic systems, climate control, insulation, power station engineering and automotive engineering. Mass transfer is the moment of molecules from one location to another i.e., from high concentration region to lower one. Mass transfer occurs through drying, membrane filtration, absorption, distillation, evaporation and precipitation. Mass transfer is useful in various disciplines such as reaction engineering, separations engineering and heat transfer engineering etc. Pramanik (2014) numerically obtained the solution for boundary layer flow induced by a stretching sheet with thermal radiation heat transfer. Makanda et al. (2015) employed a bi-variate quasilinearization method to study the thermal radiation effects on MHD slip motion due to a circular cylinder with convection and viscous dissipation. Krishna et al. (2017) examined the effects of thermal radiation on the flow of Cu-water and AlCu-water towards a deformable geometry.

Ibrahim et al. (2010) presented the results for concentration profiles of power-law fluid with thermal diffusion. The impact of cross-diffusion, radiation and thermophoresis on heat transfer MHD flow towards a wedge was analysed by Pal and Mondal (2013). Reddy et al. (2017) compared the results for the flows of two distinct non-Newtonian fluids (Casson and Maxwell fluids) with frictional heat, Soret and Dufour effects.

Raptis and Massalas (1998) studied the radiative viscous flows with unsteadiness. Yih (1997) employed Keller-box algorithm to vet the mass transfer impact on the flows via surface. The numerical solution for the physical properties of the radiative fluid towards a flat surface in the presence of Joule heating was scrutinized by Ibrahim (2013). Reddy et al. (2016) observed that heat transfer rate in spherically shaped nano particles is efficiently higher than that of cylindrical shaped nano particles when the flow is across a permeable flat plate. Rana et al. (2012) discussed the fluid motion across an inclined surface with buoyancy forces. The impression of uneven heat sink/source on Jeffrey-nanofluid flow caused by stretching sheet was proposed by Avinash et al. (2017). Prakash et al. (2014) discussed the time dependent electrically conducting flows due to an accelerated vertical wavy plate with the existence of radiation and Dufour effects. Ahmed et al. (2010) focused their investigation towards the fluid flow caused by a stretching plate. Chauhan and Rastogi (2012) adopted the Crank-Nicolson finite difference method to solve the boundary layer flow past an accelerating surface accounting Hall effects and slip boundary conditions. A

numerical investigation conducted by Aruna et al. (2015) consists of cross diffusion impacts on MHD flow (unsteady) towards a wavy plate.

From the above all literature we found that nobody reported the characteristics of heat and mass transfer on time dependent flow of non-Newtonian fluid towards an accelerated vertical wavy plate in the presence of radiation, heat source, magnetic field and thermo diffusion effects. Hence motivated by the applications and significance of this type of studies, we make an attempt to analyse such flows. In present days, the radiation heat transfer plays an important key role in chemical industries, medicine and climate control etc. So, in present perusal we investigate the impact of Soret number on radiative Casson fluid flow through a wavy plate with the help of analytical solution.

## 2. Formulation of the Problem

We consider a Cartesian coordinate system ( $xy$ –plane) to represent the flow of Casson fluid towards an accelerated vertical wavy plate. The flow is unsteady. The plate is taken along  $x$ –axis. A magnetic field ( $B_0$ ) is applied uniformly along the direction of  $y$ –axis, which is taken perpendicular to plate as shown in Fig. 1. By the influence of radiation, heat source and thermo diffusion are accounted while constructing the governing equations. The effects of chemical reaction and viscous dissipation are omitted.

The rheological equation for the Cauchy stress tensor of Casson fluid can be written as

$$\tau_{ij} = \begin{cases} 2\left(\mu_B + p_y / \sqrt{2\pi}\right) e_{ij}, & \pi > \pi_c \\ 2\left(\mu_B + p_y / \sqrt{2\pi_c}\right) e_{ij}, & \pi < \pi_c \end{cases} .$$

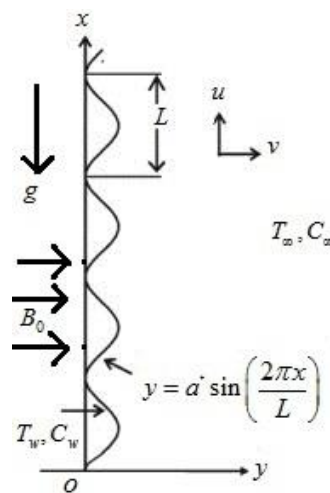


Fig. 1. Physical model of the problem

According to the assumptions mentioned above, the following are the partial differential equations representing the flow situation (Ibrahim et al., 2010; Prakash et al., 2014; Pushpalatha et al., 2017).

$$\frac{\partial u}{\partial x} + \frac{\partial v}{\partial y} = 0 \quad (1)$$

$$\begin{aligned} \frac{\partial u}{\partial t^*} + \left( u \frac{\partial u}{\partial x} + v \frac{\partial u}{\partial y} \right) = & -\frac{1}{\rho} \frac{\partial p}{\partial x} + (1 + \beta^{-1}) \nu \left( \frac{\partial^2 u}{\partial x^2} + \frac{\partial^2 u}{\partial y^2} \right) \\ & - \frac{\sigma B_0^2}{\rho} u + g \beta_T (T - T_\infty) + g \beta_C (C - C_\infty) \end{aligned} \quad (2)$$

$$\frac{\partial T}{\partial t^*} + \left( u \frac{\partial T}{\partial x} + v \frac{\partial T}{\partial y} \right) = \frac{k}{\rho C_p} \left( \frac{\partial^2 T}{\partial x^2} + \frac{\partial^2 T}{\partial y^2} \right) - \frac{Q_0 (T - T_\infty)}{\rho C_p} - \frac{1}{\rho C_p} \left( \frac{\partial q}{\partial x} + \frac{\partial q}{\partial y} \right) \quad (3)$$

$$\frac{\partial C}{\partial t^*} + \left( u \frac{\partial C}{\partial x} + v \frac{\partial C}{\partial y} \right) = D \left( \frac{\partial^2 C}{\partial x^2} + \frac{\partial^2 C}{\partial y^2} \right) + \frac{DK_T}{T_m} \frac{\partial^2 T}{\partial y^2} \quad (4)$$

The boundary conditions which fit for the current inspection are (Prakash et al., 2014)

$$\left. \begin{aligned} t^* \leq 0: & \quad u = 0, T = T_\infty, C = C_\infty, \quad \forall y \\ t^* > 0: & \quad u = u_p, \frac{\partial T}{\partial y} = B_1 T_w, \frac{\partial C}{\partial y} = B_1 C_w, \quad \text{when } y = a^* \sin \left( \frac{2\pi x}{L} \right) \\ u \rightarrow u_\infty = & \quad u_0 (1 + \varepsilon e^{n^* t^*}), \quad T_w \rightarrow T_\infty, \quad C_w \rightarrow C_\infty, \end{aligned} \right\} \quad (5)$$

In view of the assumptions made above, the continuity equation takes the below form.

$$\frac{\partial u}{\partial x} = 0 \quad (6)$$

The exponential form of suction velocity will be

$$v = -V_0 \left( 1 + \varepsilon A e^{n^* t^*} \right), \quad A > 0 \quad (7)$$

Here  $V_0$  is a scale of suction velocity. In the exterior of the boundary layer, Eqn. (2) becomes

$$-\frac{1}{\rho} \frac{dp}{dx} = \frac{du_\infty}{dt^*} + \frac{\sigma B_0^2}{\rho} u_\infty = B \quad (8)$$

So that the pressure  $p$  is independent of  $y$ .

The radiative heat flux is given by

$$\frac{\partial q}{\partial Y} = 4(T_0 - T)I' \quad (9)$$

Where  $I' = \int_0^{\infty} K_{\lambda w} \frac{\partial e_{b\lambda}}{\partial T} d\lambda$ ,  $K_{\lambda w}$  is the radiation absorption coefficient at the plate and  $e_{b\lambda}$  is Planck's function.

We make use of the below said non-dimensional quantities to convert the governing PDEs as ODEs.

$$\left. \begin{aligned} U &= \frac{u}{U_0}, V = \frac{v}{V_0}, X = \frac{x}{L}, Y = \frac{V_0 y}{\nu}, U_{\infty} = \frac{u_{\infty}}{U_0}, t = \frac{V_0^2 t^*}{\nu}, n = \frac{n^* \nu}{V_0^2}, \theta = \frac{T - T_{\infty}}{T_w - T_{\infty}}, \\ Sc &= \frac{\nu}{D}, \phi = \frac{C - C_{\infty}}{C_w - C_{\infty}}, M = \frac{\sigma B_0^2 \nu}{\rho V_0^2}, Sr = \frac{DK_T (T_w - T_{\infty})}{T_m \nu (C_w - C_{\infty})}, Gr = \frac{\nu g \beta_T (T_w - T_{\infty})}{U_0 V_0^2}, \\ Pr &= \frac{\mu C_p}{k}, Gc = \frac{\nu g \beta_c (C_w - C_{\infty})}{U_0 V_0^2}, Q_h = \frac{Q_0 \nu}{\rho C_p V_0^2}, F = \frac{4I'}{\rho C_p V_0}, U_p = \frac{u_p}{U_0}, \\ B_1 &= \frac{V_0}{\nu}, h = a \sin(2\pi X), \end{aligned} \right\} \quad (10)$$

Using Eqn. (10) the basic Eqs. (2) to (4) takes the following non-dimensional form. Also, they are now ordinary diff. equations.

$$\frac{\partial U}{\partial t} - (1 + \epsilon A e^{mY}) \frac{\partial U}{\partial Y} = \left(1 + \frac{1}{\beta}\right) \frac{\partial^2 U}{\partial Y^2} - MU + Gr\theta + Gc\phi + B \quad (11)$$

$$\frac{\partial \theta}{\partial t} - (1 + \epsilon A e^{mY}) \frac{\partial \theta}{\partial Y} = \frac{1}{Pr} \frac{\partial^2 \theta}{\partial Y^2} - (\alpha_T + F)\theta \quad (12)$$

$$Sc \frac{\partial \phi}{\partial t} - Sc(1 + \epsilon A e^{mY}) \frac{\partial \phi}{\partial Y} = \frac{\partial^2 \phi}{\partial Y^2} + Sc Sr \frac{\partial^2 \theta}{\partial Y^2} \quad (13)$$

The boundary conditions become,

$$t \leq 0 : U = 0, \theta = 0, \phi = 0, \quad \text{for all } Y \quad (14)$$

$$t > 0: U = U_p, \frac{\partial \theta}{\partial y} = 1, \frac{\partial \phi}{\partial y} = 1 \quad \text{at } Y = h \quad (15)$$

$$U \rightarrow U_\infty = 1 + \epsilon e^{nt}, \theta \rightarrow 0, \phi \rightarrow 0, \quad \text{as } Y \rightarrow \infty \quad (16)$$

### 3. Problem Solution

The coupled Eqs. (11) – (13) can be solved analytically by using perturbation method and then reducing them into a set of dimensionless ODEs. This can be possible only when the amplitude of oscillations  $\epsilon (\ll 1)$  is very small. We can assume the solutions of the flow are velocity  $U$ , temperature  $\theta$  and concentration  $\phi$  in the neighbourhood of the surface as,

$$U(y, t) = U_0(y) + \epsilon e^{nt} U_1(y) + o(\epsilon^2) \quad (17)$$

$$\theta(y, t) = \theta_0(y) + \epsilon e^{nt} \theta_1(y) + o(\epsilon^2) \quad (18)$$

$$\phi(y, t) = \phi_0(y) + \epsilon e^{nt} \phi_1(y) + o(\epsilon^2) \quad (19)$$

On substituting the expressions in Eqs. (17) – (19) into Eqs. (11) – (13), equating harmonic and non-harmonic terms, and neglecting the higher-order terms of  $o(\epsilon^2)$ , we get the following set of equations for  $U_0, \theta_0, \phi_0$  and  $U_1, \theta_1, \phi_1$ .

$$A_{14} U_0'' + U_0' - M U_0 = Gr \theta_0 + Gc \phi_0 + B \quad (20)$$

$$A_{14} U_1'' + U_1' - (M + n) U_1 = Gr \theta_1 + Gc \phi_1 + A U_0' \quad (21)$$

$$\theta_0'' + Pr \theta_0' - Pr(\alpha_r + F) \theta_0 = 0 \quad (22)$$

$$\theta_1'' + A Pr \theta_1' + Pr \theta_1' - Pr(\alpha_r + F + n) \theta_1 = 0 \quad (23)$$

$$\phi_0'' + Sc \phi_0' = -Sr Sc \theta_0'' \quad (24)$$

$$\phi_1'' + Sc \phi_1' - n Sc \phi_1 = -(Sr Sc \theta_1'' + A Sc \phi_0') \quad (25)$$

With the help of Eqs. (14)-(16) and (17)-(19), we acquire

$$U_0 = U_p, U_1 = 0, \theta_0' = 1, \theta_1' = 0, \phi_0' = 1, \phi_1' = 0, \quad \text{at } Y = h \quad (26)$$

$$U_0 = 1, U_1 = 1, \theta_0 \rightarrow 0, \theta_1 \rightarrow 0, \phi_0 \rightarrow 0, \phi_1 \rightarrow 0, \quad \text{as } Y \rightarrow \infty \quad (27)$$

Finally solutions for  $U_0, \theta_0, \phi_0$  and  $U_1, \theta_1, \phi_1$  are given by,

$$U_0 = A_{20}e^{-A_{15}Y} + A_{19} + (A_{16} + A_{18})e^{-A_4Y} + A_{17}e^{-ScY} \quad (28)$$

$$U_1 = A_{31}e^{-A_{21}Y} + A_{28}e^{-A_{15}Y} + A_{24}e^{-A_8Y} + (A_{22} + A_{25})e^{-A_3Y} + \\ (A_{23} + A_{26} + A_{29})e^{-A_4Y} + (A_{27} + A_{30})e^{-ScY} \quad (29)$$

$$\theta_0 = A_2e^{-A_4Y} \quad (30)$$

$$\theta_1 = A_5e^{-A_3Y} + A_4e^{-A_4Y} \quad (31)$$

$$\phi_0 = A_7e^{-ScY} + A_6e^{-A_4Y} \quad (32)$$

$$\phi_1 = A_{13}e^{-A_8Y} + A_9e^{-A_3Y} + (A_{10} + A_{12})e^{-A_4Y} + A_{11}e^{-ScY} \quad (33)$$

On substituting the solutions of  $U_0, U_1, \theta_0, \theta_1, \phi_0$  and  $\phi_1$  obtained from Eqs. (28) – (33) into Eqs. (17)–(19), we procure the following.

$$U(Y, t) = \epsilon e^{nt} \left[ A_{31}e^{-A_{21}Y} + A_{28}e^{-A_{15}Y} + A_{24}e^{-A_8Y} + (A_{22} + A_{25})e^{-A_3Y} + \right. \\ \left. (A_{23} + A_{26} + A_{29})e^{-A_4Y} + (A_{27} + A_{30})e^{-ScY}, \right] + A_{20}e^{-A_{15}Y} + \\ A_{19} + (A_{16} + A_{18})e^{-A_4Y} + A_{17}e^{-ScY} \quad (34)$$

$$\theta(Y, t) = [A_2e^{-A_4Y}] + \epsilon e^{nt} [A_5e^{-A_3Y} + A_4e^{-A_4Y}] \quad (35)$$

$$\phi(Y, t) = [A_7e^{-ScY} + A_6e^{-A_4Y}] + \epsilon e^{nt} [A_{13}e^{-A_8Y} + A_9e^{-A_3Y} + (A_{10} + A_{12})e^{-A_4Y} + A_{11}e^{-ScY}] \quad (36)$$

The expressions for  $Sh, Nu$  and  $C_F$  are obtained as

$$C_F = - \left\{ \begin{aligned} &A_2A_{15} + A_1(A_{16} + A_{18}) + ScA_{17} + \epsilon e^{nt} (A_{21}A_{31} + A_{15}A_{28} + A_8A_{24} \\ &+ A_3(A_{22} + A_{25}) + A_1(A_{23} + A_{26} + A_{29}) + Sc(A_{27} + A_{30})) \end{aligned} \right\} \quad (37)$$

$$Nu = A_1A_2 + \epsilon e^{nt} (A_3A_5 + A_1A_4) \quad (38)$$

$$Sh = ScA_7 + A_1A_6 + \epsilon e^{nt} (A_8A_{13} + A_3A_9 + A_1(A_{10} + A_{12}) + ScA_{11}) \quad (39)$$

#### 4. Results and Discussion

The graphs are plotted for the set of analytical solutions in Eqs. (34) - (36) with respect to the boundary conditions given in Eqs. (14) - (16) by using MATLAB bvp4c package. The graphs are drawn for the pertinent parameters namely Casson parameter ( $\beta$ ), Soret number ( $Sr$ ), a constant ( $h$ ), moving velocity of the plate ( $U_p$ ), mass Grashof number ( $Gc$ ), heat absorption parameter ( $Q_h$ ), radiation parameter ( $F$ ), thermo diffusion parameter ( $Sr$ ) and Schmidt number ( $Sc$ ) etc as shown in Figs. 2-11. In the present analysis, we presumed the parametric values as constant in our entire analysis  $Gr = 5$ ,  $Gc = 5$ ,  $n = 10$ ,  $Pr = 7$ ,  $Sc = 0.6$ ,  $M = 2$ ,  $U_p = 0.2$ ,  $F = 2$ ,  $\alpha_r = 0.5$ ,  $t = 0.2$ ,  $h = 0.2$ ,  $\varepsilon = 0.2$ ,  $Sr = 0.5$ .

Fig. 2 represents the variation in velocity for different values of Casson parameter ( $\beta$ ). An upsurge in the magnitude of Casson parameter restricts the flow velocity. Because of increasing values of  $\beta$  produces a high resistance in the flow due to the higher viscosity of the fluid.

The impact of Soret parameter ( $Sr$ ) on velocity profiles is discerned through Fig. 3. We eye that enlarging values of  $Sr$  inflates the thickness of velocity boundarylayer. Fig. 4 depicts the impact of varying values of  $h$  on velocity profiles. It can be found from Fig. 4 that the swelling values of  $h$  raises the flow velocity. Fig. 5 is sketched for studying the effect of moving velocity of the plate on fluid velocity. It is clear that the growing the values of moving velocity of the plate ( $U_p$ ) decays velocity profiles. Because an enhancement in  $U_p$  opposes the motion of Casson fluid. Fig. 6 displays the impact of mass Grashof number ( $Gc$ ) on velocity. We observe a growth in fluid velocity with the growing values of  $Gc$ . Physically, the relation between buoyancy forces to viscous forces is termed as Grashof number. So the momentum boundary layer enhances owing to buoyancy force at the wavy plate. This outcome concurs with that of Prakash et al. (2014).

Figs. 7 and 8 reveal the impact of heat absorption parameter ( $Q_h$ ) and radiation parameter ( $F$ ) on temperature profiles respectively. From these Figures, we notice that temperature decreases with increase in either heat absorption parameter  $Q_h$  or Radiation parameter  $F$ . Because of enhancing in heat absorption parameter imbibe more heat from the fluid, which leads to shrinks the layer thickness. This result coincides with the earlier result found by Prakash et al. (2014). Already we discussed that radiation is the emission of waves, which carry heat away from the flow. As a consequence temperature will be depressed. Fig. 9 represents the impact of  $h$  on temperature of the fluid. Because of it is already observed from Fig. 4 that the swelling values of  $h$  helps to move the fluid faster along the plate. As a result of temperature profiles will be raised.

Fig. 10 and 11 are sketched to know the influence of Soret number ( $Sr$ ) and Schmidt number ( $Sc$ ) on concentration profiles respectively. We found that increase in  $Sr$  depreciates the concentration distribution. But, an opposite trend is noticed in the same distribution for higher

values of  $Sc$ . The reasons are i) Increase in  $Sr$  means that transformation of concentration gradients to thermal field ii) Schmidt number is proportional to the rate of viscous diffusion.

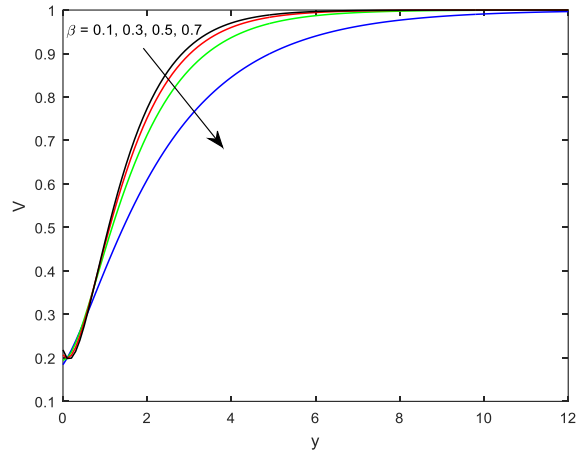


Fig. 2. Profiles of  $V$  with a change in  $\beta$

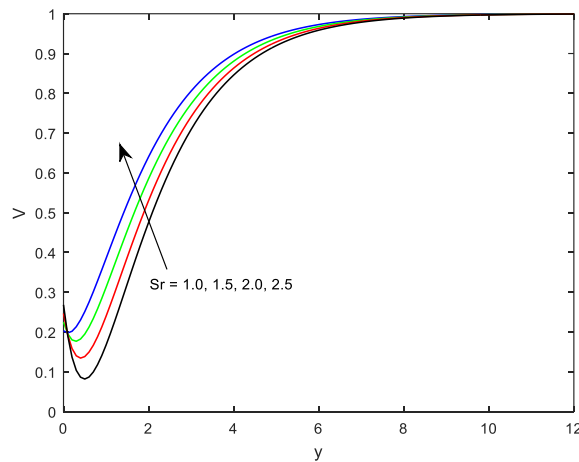


Fig. 3. Profiles of  $V$  with a change in  $Sr$

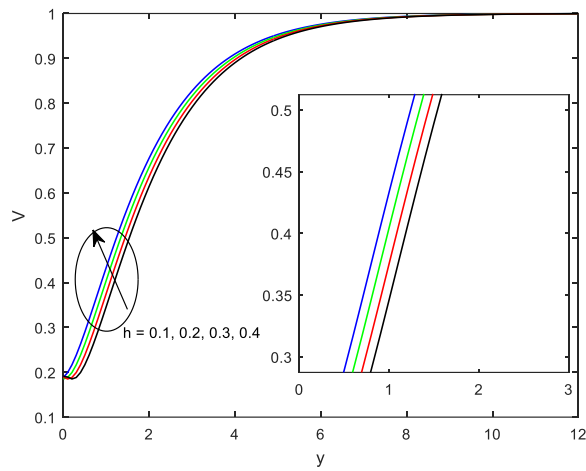


Fig. 4. Profiles of  $V$  with a change in  $h$

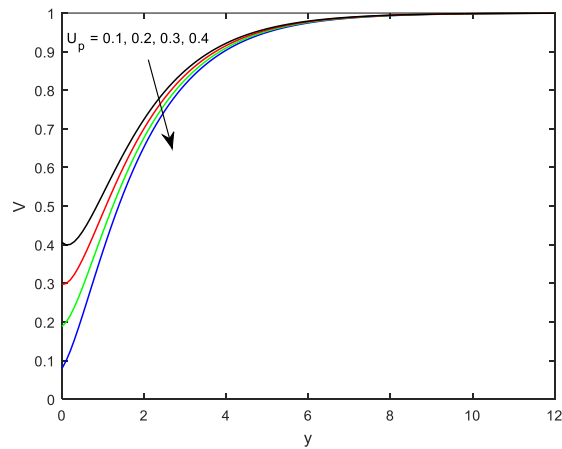


Fig. 5. Profiles of  $V$  with a change in  $U_p$

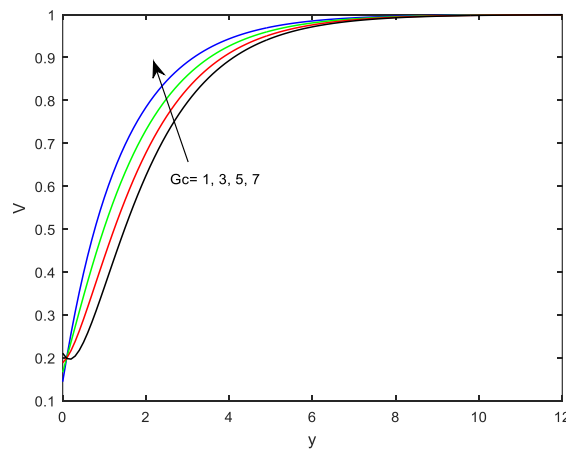


Fig. 6. Profiles of  $V$  with a change in  $Gc$

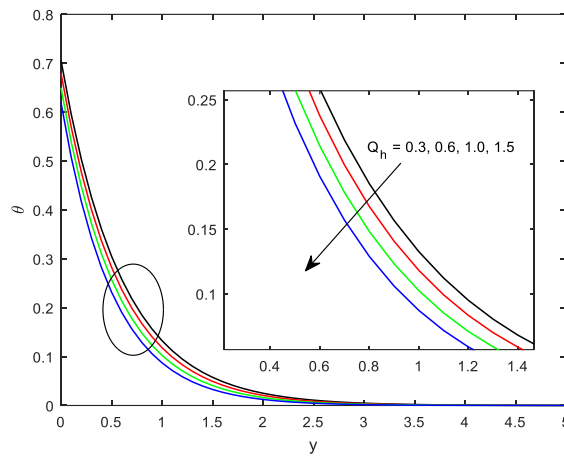


Fig. 7. Profiles of  $\theta$  with a change in  $Q_h$

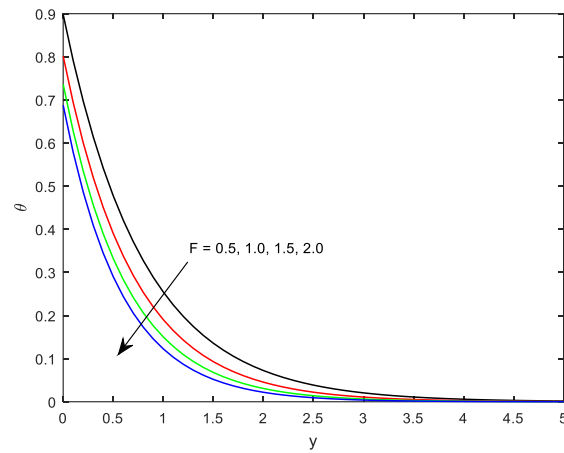


Fig. 8. Profiles of  $\theta$  with a change in  $F$

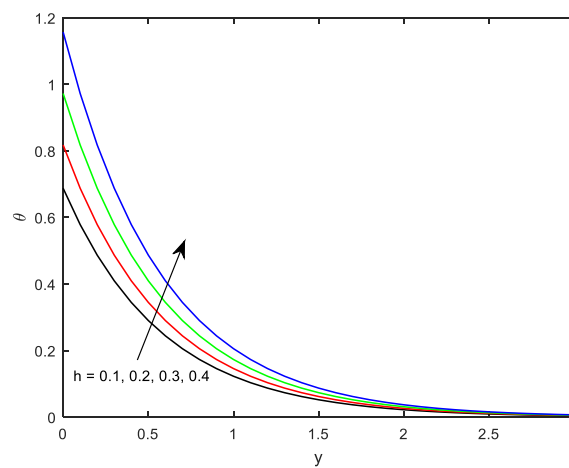


Fig. 9. Profiles of  $\theta$  with a change in  $h$

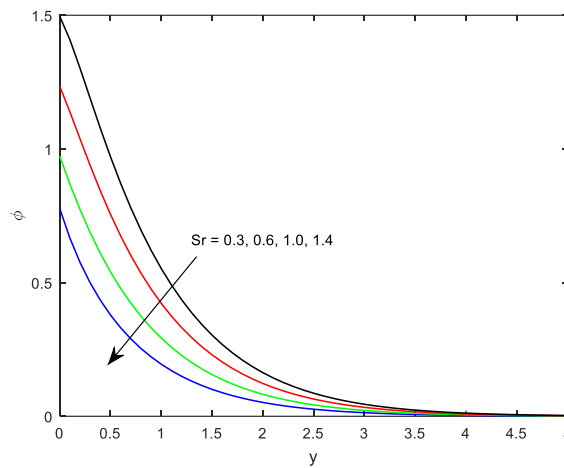


Fig. 10. Profiles of  $\phi$  with a change in  $Sr$

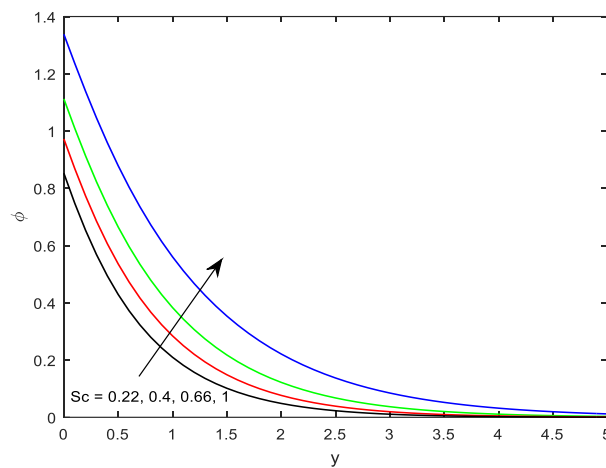


Fig. 11. Profiles of  $\phi$  with a change in  $Sc$

Table1. Effect of various physical parameters on Skin friction ( $C_F$ )

$M$	$\beta$	$Gr$	$F$	$Sr$	$Pr$	$U_p$	$C_F$
1							0.6588
2							1.0344
3							1.3476
	0.2						1.7649
	0.3						3.2066
	0.4						4.8983
		1					0.7074
		3					0.6588

		5					0.6103
			1.0				0.6588
			1.5				0.2297
			2.0				0.1488
				1			0.9379
				2			1.7589
				3			2.5799
					4.0		0.1243
					7.2		0.1341
					11.4		0.1389
						0.2	0.6588
						0.5	0.5533
						0.8	0.4477

Table 2. Effect of various physical parameters on Nusselt number ( $Nu$ )

$Gr$	$F$	$Pr$	$\alpha_T$	$Nu$
1				2.1894
3				2.2962
5				2.2971
	1.0			2.2528
	1.5			3.1072
	2.0			3.7978
		4.0		1.1437
		7.2		1.6582
		11.4		2.0690
			1	2.3538
			3	2.8779
			5	3.3160

Table 3. Effect of various physical parameters on Sherwood number ( $Sh$ )

$F$	$\alpha_T$	$Sc$	$Sr$	$Sh$
1.0				1.3513
1.5				1.7141
2.0				1.9935
	1			1.3476
	3			1.3327
	5			1.3236

		0.2		0.7589
		0.4		1.0898
		0.6		1.3513
			1	1.5152
			2	1.0162
			3	0.5198

The numerical values of  $C_f$ ,  $Nu$  and  $Sh$  with varying values of pertinent parameters for the flow across a vertical wavy plate are represented in Table 1, 2 and 3 respectively. From Table 1, we observe that an increment in Skin friction with boosting values of the magnetic parameter ( $M$ ), Casson parameter ( $\beta$ ), Soret number ( $S_r$ ) and Prandtl number ( $Pr$ ) but an opposite result is noticed in case of Grashof number ( $Gr$ ), radiation parameter ( $F$ ) and moving velocity of the plate ( $U_p$ ). From Table 2, it is clear that an increase in Grashof number ( $Gr$ ), radiation parameter ( $F$ ), Prandtl number ( $Pr$ ) and heat source parameter ( $\alpha_T$ ) inflate the heat transfer rate. In Table 3, we eyed that ascending values of either radiation parameter ( $F$ ) or Schmidt number ( $Sc$ ) enhances the Sherwood number but it is diminished by Soret number ( $S_r$ ) and heat source parameter ( $\alpha_T$ ).

## 5. Conclusions

We investigate the combined impacts of Soret number and radiation on time dependent flow of Casson fluid over an accelerated vertical wavy plate in the presence of Lorentz force. The chief conclusions in this investigation are as follows.

- The viscosity of the fluid and partial slip velocity near the surface causes a decay in the velocity of the fluid.
- Higher values of  $Sc$  develops a concentration in the boundary layer but the result is reversed with  $S_r$ .
- The rate of heat transfer increases with  $Pr$ ,  $F$ ,  $Gr$  &  $\alpha_T$ .
- A raise in radiation helps to increase the rate of heat and mass transfer but declines the Skin friction.

## Appendix

$$A_1 = \frac{Pr + \sqrt{Pr^2 + 4Pr(\alpha_T + F)}}{2}, A_2 = \frac{-e^{A_1 h}}{A_1}, A_3 = \frac{Pr + \sqrt{Pr^2 + 4Pr(\alpha_T + F + n)}}{2},$$

$$A_4 = \frac{AA_1 A_2 Pr}{A_1^2 - Pr(A_1 + \alpha_T + F + n)}, A_5 = \frac{-A_4 A_1 e^{-A_1 h}}{A_3 e^{-A_3 h}}, A_6 = \frac{-Sr Sc A_2 A_1^2}{A_1^2 - Sc A_1},$$

$$\begin{aligned}
 A_7 &= -\left(\frac{1 + A_6 A_1 e^{-A_1 h}}{Sc e^{-Sch}}\right), \quad A_8 = \frac{Sc + \sqrt{Sc^2 + 4Scn}}{2}, \quad A_9 = \frac{-SrScA_3 A_3^2}{A_3^2 - Sc(A_3 + n)}, \\
 A_{10} &= \frac{-SrScA_4 A_1^2}{A_1^2 - Sc(A_1 + n)}, \quad A_{11} = \frac{AA_7 Sc^2}{Sc^2 - Sc(Sc + n)}, \quad A_{12} = \frac{AA_1 A_6 Sc}{A_1^2 - Sc(A_1 + n)}, \\
 A_{13} &= \frac{-1}{A_8 e^{-A_8 h}} \left[ A_9 A_3 e^{-A_3 h} + (A_{10} + A_{12}) A_1 e^{-A_1 h} + Sc A_{11} e^{-Sch} \right], \\
 A_{14} &= 1 + \frac{1}{\beta}, \quad A_{15} = \frac{A_{14} + \sqrt{A_{14}^2 + 4MA_{14}}}{2}, \quad A_{16} = \frac{-GrA_2 A_{14}}{A_1^2 - A_{14}(A_1 + M)}, \\
 A_{17} &= \frac{-GcA_7 A_{14}}{Sc^2 - A_{14}(Sc + M)}, \quad A_{18} = \frac{-GcA_6 A_{14}}{A_1^2 - A_{14}(A_1 + M)}, \quad A_{19} = \frac{B}{M}, \\
 A_{20} &= \frac{-1}{e^{-A_{15} h}} \left[ U_p - (A_{16} + A_{18}) e^{-A_1 h} + A_{17} e^{-Sch} + A_{19} \right], \quad A_{21} = \frac{A_{14} + \sqrt{A_{14}^2 + 4A_{14}(M + n)}}{2}, \\
 A_{22} &= \frac{-GrA_{14} A_5}{A_3^2 - A_{14}(A_3 + M + n)}, \quad A_{23} = \frac{-GrA_{14} A_4}{A_1^2 - A_{14}(A_1 + M + n)}, \quad A_{24} = \frac{-GcA_{14} A_{13}}{A_8^2 - A_{14}(A_8 + M + n)}, \\
 A_{25} &= \frac{-GcA_{14} A_9}{A_3^2 - A_{14}(A_3 + M + n)}, \quad A_{26} = \frac{-GcA_{14}(A_{10} + A_{12})}{A_1^2 - A_{14}(A_1 + M + n)}, \quad A_{27} = \frac{-GcA_{14} A_{11}}{Sc^2 - A_{14}(Sc + M + n)}, \\
 A_{28} &= \frac{AA_{14} A_{15} A_{20}}{A_{15}^2 - A_{14}(A_{15} + M + n)}, \quad A_{29} = \frac{AA_1 A_{14}(A_{16} + A_{18})}{A_1^2 - A_{14}(A_1 + M + n)}, \\
 A_{30} &= \frac{AA_{14} A_{17} Sc}{Sc^2 - A_{14}(Sc + M + n)}, \quad A_{31} = \frac{-1}{e^{-A_{21} h}}, \\
 A_{31} &= \frac{-1}{e^{-A_{21} h}} \left[ A_{28} e^{-A_{15} h} + A_{24} e^{-A_8 h} + (A_{22} + A_{25}) e^{-A_3 h} \right. \\
 &\quad \left. + (A_{23} + A_{26} + A_{29}) e^{-A_1 h} + (A_{27} + A_{30}) e^{-Sch} \right].
 \end{aligned}$$

## References

- Ahmad, N., Siddiqui, Z. U., & Mishra, M. K. (2010). Boundary layer flow and heat transfer past a stretching plate with variable thermal conductivity. *International Journal of Non-Linear Mechanics*, 45(3), 306-309.
- Aruna, G., Varma, S. V., & Raju, R. S. (2015). Combined influence of Soret and Dufour effects on unsteady hydromagnetic mixed convective flow in an accelerated vertical wavy plate through a porous medium. *International Journal of Advances in Applied Mathematics and Mechanics*, 3(1), 122-134.
- Avinash, K., Sandeep, N., & Makinde, O. D. (2017). Non-uniform heat source/sink effect on liquid film flow of Jeffrey nanofluid over a stretching sheet. *Diffusion Foundations*, 11, 72-83.

- Chauhan, D. S., & Rastogi, P. (2012). Hall effects on MHD slip flow and heat transfer through a porous medium over an accelerated plate in a rotating system. *International Journal of Nonlinear Science*, 14(2), 228-236.
- Hameed, M., & Nadeem, S. (2007). Unsteady MHD flow of a non-Newtonian fluid on a porous plate. *Journal of Mathematical Analysis and Applications*, 325(1), 724-733.
- Han, S., Zheng, L., Li, C., & Zhang, X. (2014). Coupled flow and heat transfer in viscoelastic fluid with Cattaneo-Christov heat flux model. *Applied Mathematics Letters*, 38, 87-93.
- Hayat, T., Shafiq, A., Alsaedi, A., & Shahzad, S. A. (2016). Unsteady MHD flow over exponentially stretching sheet with slip conditions. *Applied Mathematics and Mechanics*, 37(2), 193-208.
- Hayat, T., Shehzad, S. A., & Alsaedi, A. (2012). Soret and Dufour effects on magnetohydrodynamic (MHD) flow of Casson fluid. *Applied Mathematics and Mechanics*, 33(10), 1301-1312.
- Ibrahim, F. S., Hady, F. M., Abdel-Gaied, S. M., & Eid, M. R. (2010). Influence of chemical reaction on heat and mass transfer of non-Newtonian fluid with yield stress by free convection from vertical surface in porous medium considering Soret effect. *Applied Mathematics and Mechanics*, 31(6), 675-684.
- Ibrahim, S. M. (2013). Effects of mass transfer, radiation, Joule heating and viscous dissipation on steady MHD marangoni convection flow over a flat surface with suction and injection. *International Journal of Engineering Mathematics*, 2013, 1-9, Article Id - 903818.
- Jayanthi, S., & Kumari, M. (2007). Effect of variable viscosity on non-Darcy free or mixed convection flow on a vertical surface in a non-Newtonian fluid saturated porous medium. *Applied Mathematics and Computation*, 186(2), 1643-1659.
- Khalid, A., Khan, I., Khan, A., & Shafie, S. (2015). Unsteady MHD free convection flow of Casson fluid past over an oscillating vertical plate embedded in a porous medium. *Engineering Science and Technology, an International Journal*, 18(3), 309-317.
- Krishna, P. M., Sandeep, N., Sharma, R. P., & Makinde, O. D. (2017). Thermal radiation effect on 3D slip motion of AlCu-water and Cu-water nanofluids over a variable thickness stretching surface. *Defect and Diffusion Forum*, 377, 141-154.
- Mahapatra, T. R., & Gupta, A. S. (2001). Magnetohydrodynamic stagnation-point flow towards a stretching sheet. *Acta Mechanica*, 152(1-4), 191-196.
- Makanda, G., Shaw, S., & Sibanda, P. (2015). Effects of radiation on MHD free convection of a Casson fluid from a horizontal circular cylinder with partial slip in non-Darcy porous medium with viscous dissipation. *Boundary Value Problems*, 1-14, DOI 10.1186/s13661-015-0333-5.
- Megahed, A. M. (2013). Variable fluid properties and variable heat flux effects on the flow and heat transfer in a non-Newtonian Maxwell fluid over an unsteady stretching sheet with slip velocity. *Chinese Physics B*, 22(9), 094701.
- Mukhopadhyay, S. (2013). Casson fluid flow and heat transfer over a nonlinearly stretching surface. *Chinese Physics B*, 22(7), 1-5, Article Id: 074701.
- Mustafa, M., Hayat, T., Pop, I., & Aziz, A. (2011). Unsteady boundary layer flow of a Casson fluid due to an impulsively started moving flat plate. *Heat Transfer*, 40(6), 563-576.
- Nadeem, S., Haq, R. U., Akbar, N. S., & Khan, Z. H. (2013). MHD three-dimensional Casson fluid flow past a porous linearly stretching sheet. *Alexandria Engineering Journal*, 52(4), 577-582.
- Pal, D., & Mondal, H. (2013). Influence of thermophoresis and Soret-Dufour on magnetohydrodynamic heat and mass transfer over a non-isothermal wedge with thermal radiation and Ohmic dissipation. *Journal of Magnetism and Magnetic Materials*, 331, 250-255.

- Prakash, J., Kumar, B. R., & Sivaraj, R. (2014). Radiation and Dufour effects on unsteady MHD mixed convective flow in an accelerated vertical wavy plate with varying temperature and mass diffusion. *Walailak Journal of Science and Technology*, 11(11), 939-954.
- Pramanik, S. (2014). Casson fluid flow and heat transfer past an exponentially porous stretching surface in presence of thermal radiation. *Ain Shams Engineering Journal*, 5(1), 205-212.
- Pushpalatha, K., Ramana Reddy, J. V., Sugunamma, V., & Sandeep, N. (2017). Numerical study of chemically reacting unsteady Casson fluid flow past a stretching surface with cross diffusion and thermal radiation. *Open Engineering*, 7, 69-76.
- Ramandevi, B., Reddy, J. V. R., Sugunamma, V., & Sandeep, N. (2017). Combined influence of viscous dissipation and non-uniform heat source/sink on MHD non-Newtonian fluid flow with Cattaneo-Christov heat flux. *Alexandria Engineering Journal*, <http://dx.doi.org/10.1016/j.aej.2017.01.026>.
- Rana, P., Bhargava, R., & Bég, O. A. (2012). Numerical solution for mixed convection boundary layer flow of a nanofluid along an inclined plate embedded in a porous medium. *Computers and Mathematics with Applications*, 64(9), 2816-2832.
- Raptis, A., & Massalas, C. V. (1998). Magnetohydrodynamic flow past a plate by the presence of radiation. *Heat and Mass Transfer*, 34(2-3), 107-109.
- Reddy, J. R., Kumar, K. A., Sugunamma, V., & Sandeep, N. (2017). Effect of cross diffusion on MHD non-Newtonian fluids flow past a stretching sheet with non-uniform heat source/sink: A comparative study. *Alexandria Engineering Journal*, <http://dx.doi.org/10.1016/j.aej.2017.03.008>.
- Reddy, J. V. R., Sugunamma, V., Sandeep, N., & Sulochana, C. (2016). Influence of chemical reaction, radiation and rotation on MHD nanofluid flow past a permeable flat plate in porous medium. *Journal of the Nigerian Mathematical Society*, 35(1), 48-65.
- Sulochana, C., Ashwinkumar, G. P., & Sandeep, N. (2016). Numerical investigation of chemically reacting MHD flow due to a rotating cone with thermophoresis and Brownian motion. *International Journal of Advanced Science and Technology*, 86, 61-74.
- Sulochana, C., Ashwinkumar, G. P., & Sandeep, N. (2016). Similarity solution of 3D Casson nanofluid flow over a stretching sheet with convective boundary conditions. *Journal of the Nigerian Mathematical Society*, 35(1), 128-141.
- Sulochana, C., Ashwinkumar, G. P., & Sandeep, N. (2016). Transpiration effect on stagnation-point flow of a Carreau nanofluid in the presence of thermophoresis and Brownian motion. *Alexandria Engineering Journal*, 55(2), 1151-1157.
- Sulochana, C., Ashwinkumar, G. P., & Sandeep, N. (2017). Boundary layer analysis of persistent moving horizontal needle in magnetohydrodynamic ferrofluid: A numerical study. *Alexandria Engineering Journal*, <http://dx.doi.org/10.1016/j.aej.2017.08.020>.
- Sulochana, C., Ashwinkumar, G. P., & Sandeep, N. (2017). Effect of frictional heating on mixed convection flow of chemically reacting radiative Casson nanofluid over an inclined porous plate. *Alexandria Engineering Journal*, <http://dx.doi.org/10.1016/j.aej.2017.08.006>.
- Sulochana, C., Ashwinkumar, G. P., & Sandeep, N. (2017). Effect of thermophoresis and Brownian moment on 2D MHD nanofluid flow over an elongated sheet. *Defect and Diffusion Forum*, 377, 111-126.
- Sulochana, C., Ashwinkumar, G. P., & Sandeep, N. (2017). Joule heating effect on a continuously moving thin needle in MHD Sakiadis flow with thermophoresis and Brownian moment. *The European Physical Journal Plus*, 132(387), 1-14.

Venkateswarlu, S., Varma, S. V. K., Kiran Kumar, R. V. M. S. S., Raju, C. S. K., & Durga Prasad, P. (2017). Radiation absorption and viscous-dissipation on MHD flow of Casson fluid over a vertical plate filled with porous layers. *Diffusion Foundation*, 11, 43-56.

Yih, K. A. (1997). The effect of transpiration on coupled heat and mass transfer in mixed convection over a vertical plate embedded in a saturated porous medium. *International Communications in Heat and Mass Transfer*, 24(2), 265-275.

Zhang, C., Zheng, L., Zhang, X., & Chen, G. (2015). MHD flow and radiation heat transfer of nanofluids in porous media with variable surface heat flux and chemical reaction. *Applied Mathematical Modelling*, 39(1), 165-181.